Final Technical Report

Mid-latitude extreme weather events are responsible for a large part of climate-related damage. Yet large uncertainties remain in climate model projections of heat waves, droughts, and heavy rain/snow events on regional scales, limiting our ability to effectively use these projections for climate adaptation and mitigation. These uncertainties can be attributed to both the lack of spatial resolution in the models, and to the lack of a dynamical understanding of these extremes.

The approach of this project is to relate the fine-scale features to the large scales in current climate simulations, seasonal re-forecasts, and climate change projections in a very wide range of models, including the atmospheric and coupled models of ECMWF over a range of horizontal resolutions (125 to 10 km), aqua-planet configuration of the Model for Prediction Across Scales and High Order Method Modeling Environments (resolutions ranging from 240 km – 7.5 km) with various physics suites, and selected CMIP5 model simulations. The large scale circulation will be quantified both on the basis of the well tested preferred circulation regime approach, and very recently developed measures, the finite amplitude Wave Activity (FAWA) and its spectrum. The fine scale structures related to extremes will be diagnosed following the latest approaches in the literature. The goal is to use the large scale measures as indicators of the probability of occurrence of the finer scale structures, and hence extreme events. These indicators will then be applied to the CMIP5 models and time-slice projections of a future climate.

a) Development of Finite Amplitude Wave Activity (FAWA) budgets and application to dynamical convergence

Much of the work in relating the large scale structures to blocking and weather extremes uses the Finite Amplitude Wave Activity (FAWA) which is defined as:

$$A(\phi_e) = \frac{1}{2\pi a \cos\phi_e}\left(\iint_{q>Q,\phi\le\phi_e(Q)} q\,dS - \iint_{q\le Q,\phi>\phi_e(Q)} q\,dS\right), \quad (1)$$

where q is a quasi-conservative quantity such as potential vorticity (PV) or geopotential height. a is Earth's radius, ϕ is latitude, dS is an area element, Q is a selected value of the q contour, and ϕ_e is the equivalent latitude corresponding to the Q contour. The direction of inequality should be adjusted according to the sign of the meridional gradient of q.

An application of the FAWA is the explanation of the poleward shift of the eddy-driven jet and weakening of the jet stream core with increasing resolution (e.g., Lu et al. 2015) that have been identified in several aquaplanet AGCMs, including the Model for Prediction Across Scales-Atmosphere (MPAS), the High Order Method Modeling Environment (HOMME), and the Community Atmospheric Model 3 (CAM3). Integrations of these models with grid resolutions of 240 km, 120 km, 60 km and 30 km show that resolutions corresponding to 60 km or smaller are needed to obtain dynamical convergence. A budget for the FAWA has been developed to diagnose the dynamical balance for the different positions of the eddy-driven jet. In this diagnostic framework, effective diffusivity, κ_{eff}, is the single most important parameter in determining the meridional distribution of the wave activity dissipation and the structure of the eddy vorticity flux. Thus the apparent convergence of the jet stream in both intensity and position is in keeping with the tendency of the convergence of the magnitude and meridional structure of effective diffusivity.

Another relevant application of an FAWA related budget is the behavior of annular modes, which are the leading modes of atmospheric variability in the extratropics. The persistence of annular modes has considerable influence on weather and extreme events. Examples include the vertical coupling between the stratosphere and the surface, duration of atmospheric blocking, and meridional meandering of jet streams. The mechanisms by which the annular mode time scales are determined have been investigated in idealized model simulations with climate change-like thermal forcings. Results indicate that the e-

folding time scales of annular modes are reduced as the mean jet moves poleward. As the timescales decrease, there is also a reduction in the number of blocked days, which implies weakened wave amplitudes on the poleward flank of the climatological jet. This suggests that as the jet moves poleward under future climate warming, the number of blocked days may decrease. Furthermore, the mechanism of jet persistence is investigated following the method outlined in Nie et al. (2014) and Lu et al. (2015). The ability of the FAWA formalism to relate wave amplitudes directly to the mean flow allows for the decomposition of eddy-momentum feedback into three components, a wave tendency term, a baroclinic source of waves, and a barotropic mixing associated with wave breaking. The decrease in eddy momentum flux feedback is best explained by the reduction in wave breaking and associated eddy mixing. This reduction in eddy mixing with jet latitude, as the eddy-driven jet separates increasingly from the subtropical jet, leads to less persistent jet variability and blocked days.

b) Spectral analysis of FAWA

A new spectral analysis of the finite-amplitude waves in the atmosphere has been developed and applied to aquaplanet model simulations. We can define a cumulative wave activity budget (related to the quantity A define in Eq. (1)) as:

$$A_{0:K} = \frac{1}{2\pi a \cos\phi_e}\left(\iint_{q_{0:K} > Q,\, \phi \le \phi_e(Q)} q_{0:K}\, dS - \iint_{q_{0:K} \le Q,\, \phi > \phi_e(Q)} q_{0:K}\, dS \right), \tag{2}$$

where K refers to the upper limit of the zonal wavenumber truncation, and q is the PV or other quasi-conserved quantity. $q_{0:K}$ refers to q obtained by retaining all wavenumbers up to and including K. Then the spectral density of wave activity at zonal wavenumber K can be defined as:

$$A_K = A_{0:K} - A_{0:(K-1)}, \tag{3}$$

Figure 1 depicts the wave activity spectrum (solid lines) using vorticity together with the EKE spectrum (dashed lines) for the latitudinal range centered about the peak of the EKE (35-45°) at the 250 hPa level in the MPAS aquaplanet simulation. *This is the first time that the wave activity spectrum has ever been computed and shown.* Characteristically identical wave activity spectra are also obtained for CAM3 and MPAS. Generally speaking, wave activity is a more discriminative metric than the traditional metrics for the midlatitude disturbances and it might present an advantage for quantifying model convergence or the lack thereof. The FAWA spectrum shows a much flatter slope than the corresponding EKE spectrum, reflecting the fact that FAWA is much more sensitive to the small scales than EKE. As such, FAWA is a much more discriminative metric for discerning the small scales and distinguishing the effect of resolution. In the forward enstrophy cascade range, the slope of wave activity spectrum is roughly half of that of the EKE spectrum, with the best fit of slope at -1.7. While it is yet to be understood why the inertial range of the wave activity has a -1.7 slope, *the much weaker dependence of wave activity spectrum on eddy scale implies that to capture the scales needed for the convergence of the effective diffusivity, models need to resolve a much broader inertial range than deemed necessary from the EKE convergence.* Resolutions with grid spacing between 60 and 30 km are required, in agreement with results previously discussed here.

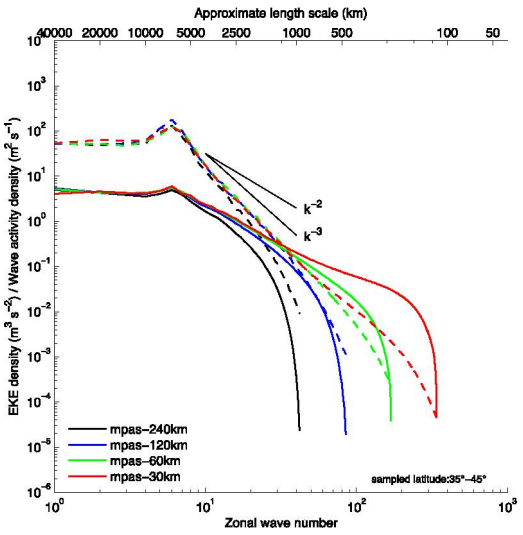

Figure 1: Spectra of finite-amplitude wave activity (solid) and EKE (dashed) sampled around the jet latitudes (between 35° and 45°) in the aquaplanet simulations of MPAS. A -3 slope and a -2 slope are drawn to guide the eyes.

c) Development of local Finite Amplitude Wave Activity (LWA) for weather extremes

While the FAWA is useful in understanding the zonal mean circulation variability, the longitudinal distribution of wave activity is critical for our understanding of extreme events on the regional scale. To that end, we have developed a local wave activity (LWA) diagnostic. More specifically, defining the eddy deviation from a mean state as $\hat{q} = q - Q$, the extension from Eq. (1) at each longitude gives

Cyclonic WA:
$$A_S(\lambda_0, \phi_e) = \frac{a}{cos\phi_e}\left(\int_{q\le Q,\ \phi\le\phi_e(Q),\ \lambda=\lambda_0} \hat{q}\, cos\phi d\phi\right) \quad (4a)$$

Anticyclonic WA:
$$A_N(\lambda_0, \phi_e) = \frac{a}{cos\phi_e}\left(\int_{q\ge Q,\ \phi\ge\phi_e(Q),\ \lambda=\lambda_0} \hat{q}\, cos\phi d\phi\right) \quad (4b)$$

Here we have separated the local anticyclonic and cyclonic wave activity at the longitude λ_0 and latitude ϕ_e. The LWA formalism is used to characterize mid-tropospheric geopotential height (Z500) in the reanalysis. Examples of the LWA during cold air outbreaks are given in Figure A2. In the Northern hemisphere, A_S describes the cyclonic wave activity residing to the south of the equivalent latitude ϕ_e, and A_N represents the anticyclonic wave activity to the north. The total wave activity $A=A_S - A_N$ takes the difference of the integral of negative $\hat{q}$ over the southward cyclonic flow and the integral of positive $\hat{q}$ over the northward anticyclonic flow, and therefore it naturally measures the waviness of the jet stream meandering and the associated cold air outbreaks in winter or heat waves in summer.

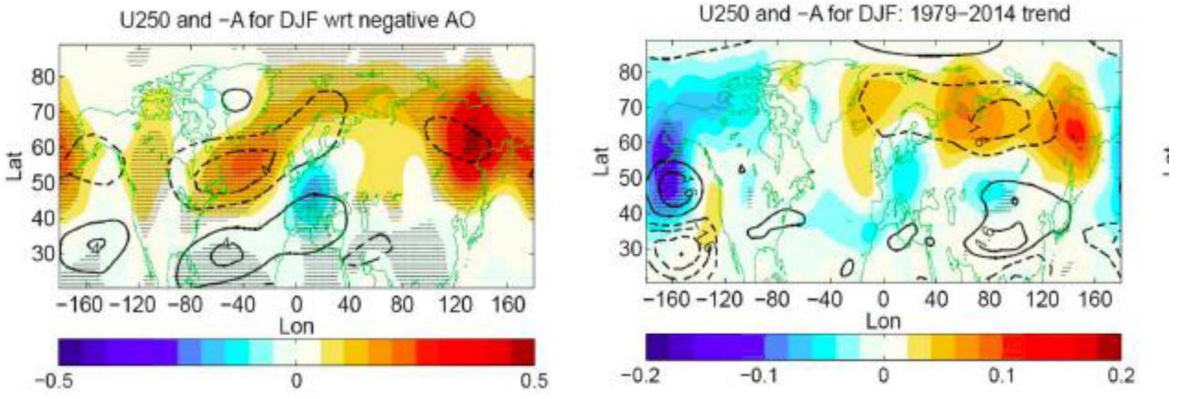

Figure 2: DJF (Contour) Zonal wind at 250 hPa and (Shading) LWA amplitude in the Era-Interim reanalysis. (Left) The regression patterns with respect to the inverted Arctic Oscillation (AO) index and (Right) the linear trends in 1979–2014.

Furthermore, the LWA climatology and its variability associated with the Arctic Oscillation (AO) agree broadly with the previously reported blocking frequency in the literature. There is a strong seasonal and spatial dependence in the trends of LWA in recent decades. Local anticorrelation is found, as expected from theory, between the zonal wind anomaly and LWA amplitude for the patterns associated with the AO as well as for the linear trends. More importantly, we found *no statistically significant evidence either in winter or in summer for a hemispheric-scale increase in wave amplitude associated with recent Arctic warming, although robust trends in wave activity can be identified at the regional scales* (see Figure 2 for DJF).

Ongoing work is extending these results from the reanalysis product to the CMIP5's 20th century and RCP scenario simulations. Comparing the observed wave amplitude trends with the CMIP5 simulations under present and future sea ice loss or RCP forcings allows to attribute the observed trends to anthropogenic forcing versus the unforced variability in the climate system. This diagnostic has also been applied to the moisture transport, which gives a quantitative measure of atmospheric rivers. The use of different reanalysis products and CMIP5 simulations will render a comprehensive description of blocking and atmospheric rivers over North America in a changing climate.

d) Linking LWA to temperature and precipitation extremes

The variability and trends of wave amplitude identified in the reanalysis and models have enabled to establish a link between the large scale circulations and temperature/precipitation extremes. Figure 3 gives an example of the composite evolution of wavy polar vortex events: the cyclonic LWA events crossing the 285° meridian and the associated temperature anomalies that are centered over the Baffin Island at lag zero. In the early phase of the wavy polar vortex events, a prominent ridge is present over the West Coast of the North American continent. Then, a low Z500 anomaly develops over Northern Quebec and leads to enhanced high-latitude reversal event frequency over Northern-Canada and Greenland. The composite that the hemispheric minimum Z500 is located over the Baffin Island at lag zero illustrates a southward displacement of the Arctic vortex, producing persistent cold spell over the Northeastern US. This work is being prepared for the Journal of climate. A parallel ongoing investigation includes the application of LWA to atmospheric moisture by bridging the large atmospheric circulation, moisture transport and precipitation extremes.

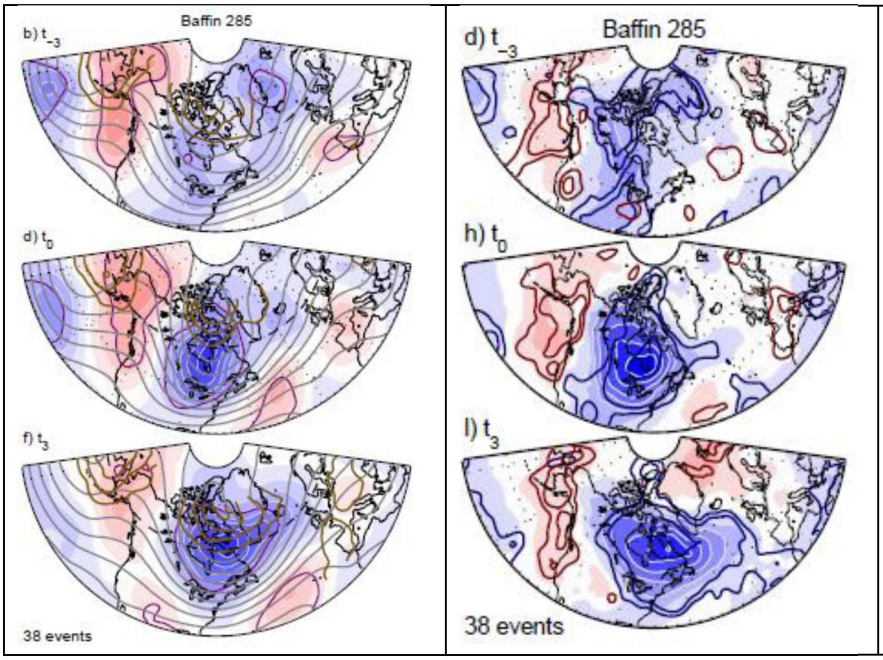

Figure 3: (Left) Composite evolution of cyclonic LWA events crossing the 285° meridian and (Right) associated temperature anomalies. Color shading in the left panel illustrates Z500 anomalies with an interval of 20m while gray contour lines illustrate the absolute Z500 field with an interval of 100m. Temperature anomalies are shown in the right panel using color shading at an interval of 1K.

Reference

- Nie, Y., Y. Zhang, G. Chen, X. Yang, and D. A. Burrows, 2014: Quantifying barotropic and baroclinic eddy feedbacks in the persistence of the Southern Annular Mode. Geophys. Res. Lett., 41, 8636–8644, doi:10.1002/2014GL062210.
- Jian Lu, Gang Chen, L. Ruby Leung, D. Alex Burrows, Qing Yang, Koichi Sakaguchi, and Samson Hagos, 2015: Toward the Dynamical Convergence on the Jet Stream in Aquaplanet AGCMs. J. Climate, 28, 6763–6782.
- Chen, G., J. Lu, D. A. Burrows, *and* L. R. Leung *(*2015*),* Local finite-amplitude wave activity as an objective diagnostic of midlatitude extreme weather, Geophys. Res. Lett., 42, 10,952–10,960, *doi:*10.1002/2015GL066959.